CO_2 photoconversion to fuels under high pressure: effect of TiO_2 phase and of unconventional reaction conditions

I. Rossetti[*,1], A. Villa[1], M. Compagnoni[1], L. Prati[1], G. Ramis[2], C. Pirola[1], C.L. Bianchi[1], W. Wang[3], D. Wang[3,4]

[1] *Dip. Chimica, Università degli Studi di Milano, INSTM Unit Milano Università and CNR-ISTM, via C. Golgi 19, 20133 Milan, Italy*

[2] *Dip. Ingegneria Chimica, Civile ed Ambientale, Università di Genova and INSTM Unit, P.le Kennedy 1, 16129 Genoa, Italy*

[3] *Institute of Nanotechnology, Karlsruhe Institute of Technology, Hermann-von-Helmholtz-Platz 1, 76344 Eggenstein-Leopoldshafen, Germany*

[4] *Institute of Nanotechnology and Karlsruhe Nano Micro Facility (KNMF), Karlsruhe Institute of Technology, Hermann-von-Helmholtz-Platz 1, 76344 Eggenstein-Leopoldshafen, Germany*

(*) corresponding author: ilenia.rossetti@unimi.it

Abstract

Artificial photosynthesis is an up to date topic for the fixation of CO_2 in form of valuable fuels. Recently, we set up an innovative concept of photoreactor to be applied to CO_2 photoreduction, enabling operation up to 20 bar. This allows to improve CO_2 solubility and to explore unconventional operating conditions for this very challenging reaction.

Following a preliminary communication, to demonstrate the validity of the approach systematic testing has been here carried out on different TiO_2 photocatalysts (anatase, rutile and anatase+rutile) doped with 0.1 wt% Au, by tuning pressure, temperature and pH. The operating conditions have been selected to maximise the production of gas phase products, *i.e*. CH_4 + H_2, with respect to liquid phase organic compounds. The present results overperform many of the recent achievements reported in the literature and throw the basis for a further optimisation of the photocatalytic material and of the photoreactor.

Keywords: CO_2 protoconversion; CO_2 protoreduction; Photoproduction of fuels; High pressure reactor; Titanium dioxide.

1 Introduction

CO_2 is among the most stable molecules, requiring high amount of energy to be activated. Photosynthesis is the most efficient way to decrease at once the concentration of two greenhouse gases, CO_2 and H_2O, the major products of combustion. This is a natural but complex process leading to a regenerated fuel by photo-irradiation. The natural process has never been fully mimicked in laboratory, due to the complexity of the enzymatic reactions involved. In spite of this, the topic is intriguing and it raised interest in the late '70s with the first attempts to fix CO_2 at least by partially reducing it to CO. However, the results were not satisfactory for different reasons. The first was a lack of knowledge on the basics of materials science for photocatalysis at that time, now partly overcome thanks to fundamental and practical advancements for different applications (e.g. photodegradation of pollutants)[1]. Another reason was that activity testing has been

carried out mostly in liquid phase, *i.e*. by dissolution of CO_2 in solvents during irradiation. The limited solubility of CO_2 in water (0.03 M at 25°C, 1 atm CO_2), especially at relatively high temperature which could improve the kinetics, always led to very poor productivity[2,3]. Some attempts with different solvents, e.g. methanol or acetonitrile (solubility 0.2 M and 0.3 M, respectively), allowed to increase solubility at the expenses of a less “green” solution, but no impressive jump of CO_2 conversion was observed. Therefore, after such explorative tests the attention on this reaction decreased, so that only a few papers on this topic may be found till that time. The topic has renewed interest recently due to pressing issues on CO_2 capture and storage, which has to be connected with its valorisation into useful compounds [4-6].

Concerning inorganic semiconductors most researchers focused on TiO_2, recently obtained in nanostructured form. Nanostructuring improved the surface area and the catalytic performance, though unacceptably depressing photo-absorption in the visible region due to blue shift of the absorption edge [4,7,8]. Indeed, for different applications the band gap proved closely related to particle size due to size quantization effects [9]. Absorption in the visible region of the solar spectrum is one of the most pressing problems to solve in order to adopt solar light for CO_2 photoactivation, since the visible portion of the solar spectrum is predominant with respect to the UV one, so far used for this application (the latter representing up to 2-3% of the solar spectrum, only [2]).

To sum up, the best productivities mostly reported up in the literature for fuels regenerated from CO_2 are attested on few mmoles/kg_{cat} h, almost exclusively under UV irradiation, a value clearly inappropriate for any practical application.

The following key topics may be evidenced:

1) Solubility limitations of CO_2 in liquid solvents, actually depressing productivity;

2) Inadequate visible light absorption to be enhanced (possibly keeping flat band potentials compatible with the redox potentials of the reactants);

3) Low efficiency in separation of photoproduced charges, to be enhanced;

4) Back-oxidation of methanol (desirable product in liquid phase) by holes, limiting the yield of liquid fuels, but opening the way to H_2 generation in gas phase;

5) Inadequate knowledge of competitive/consecutive reactions.

At least to our knowledge, the best results up to now published on the topic have been proposed by Corma and Garcia [5] over basic zeolites. They reported 100% selectivity to methane, with a production rate of 77 mmol/h kg_{cat} , accompanied by *ca.* 10 times higher productivity of H_2 (irradiation conditions: 184 nm, 86 W/m^2). Interesting results as for methanol production have been also recently reported under visible light irradiation over hexanuclear molybdenum clusters [10].

Most papers report very limited CH_4 productivity, below 5 mmol/h kg_{cat} [11-16] and the majority of the reports do not include the quantification of H_2. Interesting productivities of CH_4, CH_3OH or HCOOH have been reported for ZnO/ZnTe, NiO-TiO_2, N-doped TiO_2 or sensitized titania [17-19], but sometimes with limited screening of possible coupled reaction mechanisms. CH_4 productivity above the average (*i.e*. *ca.* 10 mmol/h kg_{cat}) has been also reported for gas phase photoreduction of CO_2 over TiO_2-GaP composite materials [20]. Some papers also evidenced problems of catalyst durability, activity curves bending towards plateau with time or decreasing visibly after the first irradiation cycles [21-23].

Further data are effectively summarised in recent review papers, including details on photoreactor engineering (see e.g. Liu et al.[24] and references therein). Actually, at present no completely feasible solution for CO_2 photoreduction is still available.

In order to answer some of these points, we searched for an active photocatalyst with enhanced electron-hole separation and we used surface plasmonic resonance given by a doping metal in order to improve catalyst photoreactivity. The photocatalytic reduction of CO_2 was carried out over three catalysts constituted by 0.1 wt% Au/TiO_2. Different polymorphs were chosen to confirm the effect of the titania structure on reactivity.

Most important from the reactor and reaction engineering point of view, we set up an innovative concept of photoreactor for the scope, able to operate up to 20 bar in liquid phase, overcoming at least in part CO_2 solubility issues and allowing to explore different temperature ranges, up to 95°C. This represents a highly innovative solution allowing to widely broaden the typical operative conditions for photocatalysis.

2 Experimental

2.1 – Catalysts preparation

$NaAuCl_4 \cdot 2H_2O$ (Aldrich, 99.99% purity), $NaBH_4$ (Fluka, purity > 96%) and urea (Aldrich, purity > 99%) were used for catalyst preparation. TiO_2 P25 from Evonik, rutile (Aldrich, 99.99% purity) and anatase (Aldrich, 99.80% purity) were compared as photocatalysts.

The samples were prepared by deposition-precipitation. 1g of TiO_2 was dispersed in distilled water (100 ml) to which urea was added (5 g). A $NaAuCl_4$ solution (Au = 0.005 mmol) was added to the support and left under vigorous stirring for 4 h at 80 °C. The catalyst was filtered and washed several times with water. The material was then suspended in distilled water and a freshly prepared solution of $NaBH_4$ (0.1 M) was added ($NaBH_4$/Au = 4 mol/mol) under vigorous stirring at room temperature. The sample was filtered, washed and dried at 100°C for 4 h. The final Au loading was 0.1 wt%. This value was chosen in order to impart some visible light absorption, sufficient metallic surface sites acting as electron scavengers, but at the same time to avoid excessive surface coverage, which would limit light absorption by the semiconductor. The metal content was checked by Atomic Absorption Spectroscopy (AAS) analysis of the filtrate, on

a Perkin Elmer 3100 instrument.

2.2 – Catalysts characterisation

X-ray diffraction (XRD) experiments were performed on a Rigaku D III-MAX horizontal-scan powder diffractometer with Cu-Kα radiation, equipped with a graphite monochromator on the diffracted beam. The crystallite size was estimated from peak half width by using the Scherrer equation with corrections for instrumental line broadening (β = 0.9).

Diffuse reflectance absorbance spectra were collected on a Jasco V570 spectrophotometer.

The TEM specimens were prepared by dispersing the catalyst powder on TEM grids coated with holey carbon film. They were examined in a FEI Titan 80-300 electron microscope equipped with CEOS image spherical aberration corrector, Fischione model 3000 high angle annular dark field (HAADF) scanning transmission electron microscopy (STEM) detector.

2.3 – Photocatalytic CO_2 reduction

The innovative photoreactor has been described elsewhere [25,26]. Briefly, the photoreactor (Soffieria Sestese Company, Sesto San Giovanni, Italy), was made of AISI 316 stainless steel. The lamp is introduced vertically in reactor axis and a magnetic stirrer ensures proper liquid mixing. The internal capacity is *ca*. 1.3 L, filled with ca. 1.2 L solution. The temperature is kept constant through a double-walled thermostatic system. A medium-pressure mercury vapor lamp (125 W) emitting in the wavelength region from 254 to 364 nm was used during testing. The harmful overheat of the lamp bulb is avoided by continuous heat removal by an air circulation system.

The catalyst, *ca*. 0.5 g, has been dispersed in demineralised and outgassed water (1-1.2 L). The suspension has been saturated with CO_2 at different temperature and pressure before starting irradiation with a 125 W medium-pressure Hg vapour lamp with a range of emission wavelengths from 254 nm to 364 nm.

Na_2SO_3 (ca. 0.85 g/L) has been used as hole scavenger. Its consumption was evaluated by iodometric titration, showing a conversion ranging from 78 to 94%. Negligible productivity has been observed without its addition. In some tests the effect of pH was also checked, by adding diluted NH_3 or HNO_3, spanning a pH range from 1.8 to 11.5.

The liquid mixture has been analysed after different reaction times by means of a Total Organic Carbon (TOC, Shimadzu 5000A) analyser and HPLC (Agilent 1220 Infinity) using a column (Alltech OA- 10308, 300 mm_7.8 mm) with UV and refractive index (Agilent 1260 Infinity) detectors. Aqueous H_3PO_4 solution (0.1 wt. %) was used as the eluent. The gas phase over the liquid has been analysed by a gaschromatograph (Agilent 7890) equipped with a TCD detector and proper set up for the quantification of H_2, CH_4 and polar/non polar light gases. Methane in gas phase has been also quantified by a micro-GC (Agilent, mod. 3000A). Every test was typically carried out for 70-100 h.

The maximum error on chromatographic analysis is 4% and 5.5% for H_2 and CH_4, respectively. Repetition of the same test under identical conditions led to an experimental error up to 10%, increasing to a maximum deviation of 19% in case of very low productivity in gas phase for H_2. Some repetitions have been carried out on recycled catalysts too, during the set up of the analysis, evidencing a productivity within the given experimental error up to three cycles. However, the tests reported in this work have been carried out on fresh aliquots of catalyst.

Light intensity has been measured using a photoradiometer model Etta-Ohm HD 2102.2.

3 Results and discussion

3.1 – Catalyst preparation and characterisation

The catalysts were prepared by adding Au by deposition precipitation in highly dispersed form on three different TiO_2 materials. The XRD patterns of all the three samples are reported in Fig. 1, which shows the presence of the different polymorphs of TiO_2 in the samples. Low reflections intensity and peak broadening were evident for the sample based on P25 TiO_2, according to its nanometric size. Au reflections were never observed due to very low loading and high dispersion achieved. The phase composition of each sample and crystal size, as determined by XRD data, are reported in Table 1. One of the samples was predominantly composed by rutile, one by anatase and the Evonik P25 sample was also used, composed by *ca.* 80% anatase. The latter was in highly dispersed nanocrystalline morphology, with TiO_2 crystal size (14-17 nm) much smaller than the other materials (50-90 nm).

Au particle size was determined from HRTEM and STEM images (Fig. 2 and 3), revealing very small and fairly narrow particle size distribution. Mean Au particle size was lower for the nanostructured P25 TiO_2, with respect to the rutile and anatase samples, (3.7, 4.1, 5.6 nm, for Au/P25, Au/rutile and Au/anatase, respectively, Table 2).

DR-UV-Vis spectroscopy was employed to assess the light absorption edge of the different samples (Fig. 4). All the samples showed the typical UV absorption of TiO_2, coupled with a plasmonic resonance band in the visible region. The absorption edge was also correlated with the band gap size of the different samples, as reported in Table 2. As expected the band gap was lower for rutile, than for P25 and anatase. However, the highest spectrum intensity was observed for the sample constituted by TiO_2 P25, demonstrating a beneficial role of nanostructuring as for absorption intensity. The same sample was also characterised by the most intense absorption in the visible region, associated

with the highest dispersion of Au particles. However, a decrease of Au particle size caused a slight blue-shift of the absorption maximum.

3.2 – Photoreduction of CO_2

To answer some of the criticisms outlined in the introduction, we developed a new concept of photoreactor, proposed by our group for the first time in this application [25]. It is represented by a device working under high pressure (up to 20 bar), in order to improve CO_2 solubility in a liquid solvent even at relatively high temperature. Preliminary testing for this application has been carried out with TiO_2 P25, doped with 0.1%wt of Au catalyst.

The possibility to saturate the system with CO_2 at different pressure and temperature induces a variation of its solubility in water, as summarised in Fig. 5 for some interesting temperature and pressure conditions. These values were calculated from solubility data as equilibrium values according to a Soave-Redlick-Kwong equation of state for the gas phase and NRTL (Non-Random Two Liquids) model to account for non-ideal behaviour in the liquid phase. As expected, the CO_2 molar fraction in liquid phase decreased at increasing temperature and increased at higher pressure. More in detail, when operating at 25°C a 16-fold increase of CO_2 concentration in liquid phase occurs upon increasing the operating pressure from 1 to 20 bar. The uptake is even higher, *i.e.* 28-times, when operating at 80°C and increasing pressure from 1 to 20 bar (Fig. 5).

These results stress the importance of exploring unconventional pressure and temperature ranges for this very challenging reaction.

In our preliminary report [25], we underlined the effect of operating conditions on photocatalytic activity. In particular, we evidenced a parallel reaction pathway, leading to the formation of liquid phase products (mainly methanol, ethanol, formic acid and formaldehyde) and methane evolving in gas phase. However, we also observed H_2 when analys-

ing the gas phase, which was commonly the predominant gaseous product of the reaction. These results were expanded here by deepening the screening of temperature/pressure effects, particularly focusing on the conditions favouring the production of gas phase products (H_2 and CH_4).

The effect of CO_2 pressure on H_2 and CH_4 productivity is reported in Fig. 6. The optimal pressure to maximise productivity of gasous products was found between 5 and 10 bar. No CO was detected under the presently selected reaction conditions. A first increase of productivity of gas phase compounds is due to the increased solubility of the reactant. However, products evolution in gas phase is hindered by further increasing pressure for thermodynamic reasons.

H_2 can be produced by direct water splitting under the selected conditions and with Au/TiO_2 catalysts, but this reaction pathway seems unlikely due to negligible O_2 concentration observed in the gas phase. Indeed, it is well known that water oxidation is by far less efficient than the photo-oxidation of organic compounds. Therefore, we added to the reaction mechanism a photoreforming step, which consumes the liquid phase organic products formed by CO_2 photoreduction to produce H_2 + CO_2, according to the reaction mechanism suggested in literature [27]:

$$CH_x + 2\ H_2O \leftrightarrows CO_2 + (x/2 + 2)\ H_2$$

Overall, the possibility to obtain H_2 (+ CH_4) as a final product of CO_2 photoreduction seems intriguing. Indeed, even though the net CO_2 consumption is lower than in a pure CO_2 photoreduction process, a valuable fuel (H_2) or gaseous fuel mixture (H_2 + CH_4) could be obtained from organic compounds deriving from CO_2 fixation. In other words: no net CO_2 emissions are released during H_2 production.

The proportions of products formation rates in liquid or gas phase were very dependent on temperature and pressure [25]. An increase of operating pressure favoured liquid organic products accumulation and was detrimental for H_2 and CH_4 productivities. By contrast, the latter were maximised when operating at intermediate pressure.

On the other hand, an increase of temperature decreases CO_2 solubility at a given pressure, but it favours kinetics and mass transfer, so that an increase of temperature usually favours the formation of a H_2/CH_4 gas mixture, at the expenses of liquid phase products. It follows that H_2 productivity is depressed by an increase of pressure due to an increase of moles, contrarily to the reaction of CH_x formation in liquid phase, which is instead improved by increasing pressure, as above stated due to improved CO_2 concentration in liquid phase.

As for CH_4 productivity, an interesting contribution has been presented by C.C. Yang et al. [28], showing the possible contribution of the decomposition of surface persisting organic compounds (coke) deriving from catalyst preparation. In the mentioned paper care is suggested for the reliable quantification of CH_4 productivity, based on isotopic exchange analyses. It should be mentioned here that a typical test among those here reported lasts *ca.* 70-100 h, thus the sample activation by irradiation, in case, occurs during the first working hours. Repeated tests on the same recycled catalyst evidenced the same H_2 and CH_4 productivities, ruling out any significant contribution of catalyst-derived carbon on products distribution.

In order to deepen the beneficial role of increasing CO_2 solubility in water, CO_2 dissolution was further enhanced by acid-base reaction, *i.e.* by adding ammonia (initial pH = 11.4). The formation of carbonates took place, but this did not turn into a higher photocatalytic activity, H_2 productivity decreasing with increasing pH. Additionally, the amount of carbon in liquid phase showed almost unaffected by pH. A decrease of pH to 1.8 was

instead detrimental leading to negligible H_2 formation, whereas methane productivity decreased from 8.5 to 6.5 mmol/h kg_{cat} when lowering pH from 11.4 to 1.8.

The effect of reaction temperature was also investigated, showing a dramatic increase of H_2 productivity with increasing temperature. Indeed, at 5 bar with the 0.1 wt% Au/P25 catalyst H_2 productivity increased by a factor of *ca*. 20 when increasing temperature from 50 to 80 °C at both pH 5.5 and 11.4 (Fig. 7). This can be mainly attributed to the improvement of kinetics with increasing temperature. This is also an important result, because it suggests that a kinetic control of the reaction may be achieved when working under high CO_2 pressure, whereas at lower pressure the reaction rate is substantially limited by dissolution equilibria.

The effect of TiO_2 structure on H_2 productivity is reported in Fig. 8 and the same trend was observed for methane production. The highest productivity for gas phase product was achieved with the TiO_2 P25 photocatalyst. This sample was characterised by the smallest crystal size and the highest Au dispersion (Tables 1 and 2), together with the smallest TiO_2 crystal size. Higher light absorption was achieved (Fig. 4) for the P25-based sample and this may be correlated to the observed higher photocatalytic activity. However, significant activity for H_2 production was also achieved with the anatase and the rutile based samples, though the latter was the least active for hydrogen and methane production. Further deepening of this point is envisaged in order to de-couple the effect of the semiconductor particle size from that of Au dispersion. A systematic investigation on this point is still in progress, but we have a first evidence that by keeping the same TiO_2 P25 support, *i.e*. fixing crystal size of the semiconductor, a decrease of Au dispersion with increasing metal loading is expected. This leads to a decrease of H_2 productivity and a contemporary increase of productivity of liquid phase products (*e.g*. formic acid).

Concerning the production of liquid phase organic compounds by CO_2 fixation, the productivity ranged between 0.6 and 1.8 gC/h kg_{cat}, by far lower than what achievable at

higher pressure (up to 110 gC/h kg_{cat} at 19 bar, 90°C), as intentionally achieved to favour gas phase products. The main product obtained for every catalyst was formic acid, followed by formaldehyde. This is in line with a consecutive reaction pathway. An increase of temperature at 6 bar from 65 to 80°C allowed to double the productivity of liquid phase products for the P25-based catalyst and to increase it by three times for the anatase-based sample. This increase of productivity was essentially due to increased formic acid concentration, the amount of acetaldehyde remaining limited. Therefore, it can be hypothesised that an increase of temperature induces a faster fixation of CO_2. The increased amount of formic acid in liquid phase, combined with higher temperature explains the higher activity for hydrogen production by photoreforming of the formic acid which is being formed.

Finally, it should be remarked that the present results were achieved with a non optimised light exposure, leading to 34 W/m^2 power in front of the light source, value rapidly decreasing to 7.6 and 2.3 W/m^2 just below and above the source, respectively. This point is presently under further optimisation and it is expected to significantly affect overall productivity.

4 Conclusions

An innovative concept of photoreactor was set up, allowing operation under pressure up to 20 bar. This system was employed to improve the solubility of CO_2 in water, one of the main limitations for CO_2 photoreduction. Interesting productivity for both liquid and gas phase photoregenerated fuels has been achieved by using different 0.1 wt% Au/TiO_2 catalysts.

The productivity of organic compounds in liquid phase increased with pressure, as the overall photocatalytic activity, due to improved CO_2 solubility in water. Physical dissolution should be enhanced instead of chemical absorption at high pH, carbonates being not involved in the photocatalytic reaction. Therefore, the set up of a pressurised photocatalytic reactor allows to explore unconventional operating conditions for this reaction and to tune them so to favour selectivity towards the desired products. In particular, operating at intermediate pressures favours the formation of gas phase products, in the form of a fuel mixture composed of H_2 + CH_4. Selectivity towards the latter compounds was also improved by increasing temperature. The highest productivity of CH_4 + H_2 was achieved at 6 bar and at the highest testing temperature (80 °C) with the 0.1 wt% Au/TiO_2 P25 sample. By contrast, under the same conditions the rutile-based ones allowed to increase the organic content in liquid phase.

Finally, the highest activity for H_2 production was attained by using 0.1 wt% Au/TiO_2 P25. Its better performance with respect to rutile and anatase was attributed to its enhanced light absorption, likely due to its nanostructured form and high metal dispersion.

Acknowledgements

This research was possible thanks to the financial support of Università degli Studi di Milano, through the measure “Piano di sviluppo d’ateneo 2014, Linea B.1” (grant attributed to I. Rossetti).

References

[1] M. Hamadanian, A. Reisi-Vanani, A. Majedi, *Mater. Chem. and Phys*., 2009, **116**, 376.

[2] M. Anpo, H. Yamashita, Y. Ichihashi, S. Ehara, J. *of Electroanalytical Chem*., 1995, **396**, 21.

[3] M. Anpo, H. Yamashita, K. Ikeue, Y. Fujii, S.G. Zhang, Y. Ichihashi, D.R. Park, Y. Suzuki, K. Koyano, T. Tatsumi, *Catal. Today*, 1998, **44**, 327.

[4] G. Centi, S. Perathoner, *Catal. Today*, 2009, **148**, 191.

[5] A. Corma, H. Garcia, *J. Catal*., 2013, **308**, 168.

[6] V.P. Indrakanti, J.D. Kubicki, H.H. Schobert, *Energy Environ. Sci*., 2009, **2**, 745.

[7] P.-Q. Wang, Y. Bai, J.-Y. Liu, Z. Fan, Y.-Q. Hu, *Catal. Commun*., 2012, **29**, 185.

[8] X. Zhang, F. Han, B. Shi, S. Farsinezhad, G. P. Dechaine, K. Shankar, *Angew. Chem. Int. Ed.*, 2012, **51**, 12732.

[9] M. Kitano, M. Matauoka, M. Ueshima, M. Anpo, *Appl. Catal. A*, 2007, **325**, 1.P. Kumar, S. Kumar, S. Cordier, S. Paofai, R. Boukherroub, S.L. Jain, *RSC Adv*., 2014, **4**, 10420.

[10] M.M. Gui, S.-P. Chai, B.-Q. Xu, A. R. Mohamed, *Solar Energy Mater. & Solar Cells*, 2014, **122**, 183.

[11] D. Kong, J.Z.Y. Tan, F. Yang, J. Zeng, X. Zhang, *Appl. Surf. Sci*., 2013, **277**, 105.

[12] M.M. Gui, W.M.P. Wong, S.-P. Chai, A.R. Mohamed, *Chem. Eng. J*., in press, DOI: http://dx.doi.org/10.1016/j.cej.2014.09.022.

[13] M. Manzanares, C. Fàbrega, J.O. Ossó, L.F. Vega, T. Andreu, J.R. Morante, *Appl. Catal. B: Environ*., 2014, **150– 151**, 57.

[14] W.-J. Ong, L.-L. Tan, S.-P. Chai, S.-T. Yong, *Dalton Trans*., 2015, **44**, 1249.

[15] L.-L. Tan, W.-J. Ong, S.-P. Chai, A.R. Mohamed, *Appl. Catal. B: Environ*., 2015, **166–167**, 251.

[16] G. Mele, C. Annese, A. De Riccardis, C. Fusco, L. Palmisano, G. Vasapollo, L. D'Accolti, *Appl. Catal. A: Gen*., 2014, **481**, 169.

[17] M.F. Ehsan, T.He, *Appl. Catal. B: Environ*., 2015, **166–167**, 345.

[18] L. Collado, A. Reynal, J.M. Coronado, D.P. Serrano, J.R. Durrant, V.A. de la Pe˜na O'Shea, *Appl. Catal. B: Environ*., in press, DOI: http://dx.doi.org/10.1016/j.apcatb.2014.09.032.

[19] G. Marcì, E.I. García-López, L. Palmisano, *Catal. Commun*., 2014, **53**, 38.

[20] B.S. Kwak, K. Vignesh, N.-K. Park, H.-J. Ryu, J.-I. Baek, M. Kang, *Fuel*, 2015, **143**, 570.

[21] B. Michalkiewicz, J. Majewska, G. Kądziołka, K. Bubacz, S. Mozia, A.W. Morawski, *J. CO_2 Utilization*, 2014, **5**, 47.

[22] O. Ola, M.M. Maroto-Valer, *J. Catal*., 2014, **309**, 300.

[23] G. Liu, N. Hoivik, K. Wangn, H. Jakobsen, *Solar Energy Materials & Solar Cells*, 2012, **105**, 53.

[24] I. Rossetti, A. Villa, C. Pirola, L. Prati, G. Ramis, *RSC Adv*., 2014, 4, 28883.

[25] C. Pirola, C. L. Bianchi, S. Gatto, S. Ardizzone, G. Cappelletti, *Chem. Eng. J.*, 2013, 225, 416.

[26] X. Yang, T. Xiao, P.P. Edwards, *Int. J. Hydrogen Energy*, 2011, **36**, 6546.

[27] C.-C. Yang, Y.-H. Yu, B. van der Linden, J.C.S. Wu, G. Mul, *J. Am. Chem. Soc*., 2010, **132**, 8398.

TABLES

Table 1*:* Crystal phases and crystallite size quantification through the Scherrer equation from XRD data.

TiO_2	*Phase composition*	*Crystallite size (nm)*
P25	Rutile 17%	17
	Anatase 83%	14
Rutile	Rutile 95%	74
	Anatase 5%	77
Anatase	Rutile 2%	54
	Anatase 98%	86

Table 2*: Au particle size distribution from HR-TEM and estimated band gap from DR-UV-Vis.*

Catalyst	*Statistical median (nm)*	*Standard Deviation (nm)*	*Bang gap (eV)*
0.1 wt% Au/P25	3.7	0.9	3.08
0.1 wt% Au/Anatase	5.6	2.0	3.24
0.1 wt% Au/Rutile	4.1	1.6	3.02

FIGURES

Fig.1: XRD patterns of different 0.1 wt% Au/TiO_2 catalysts. From bottom up, P25, rutile and anatase.

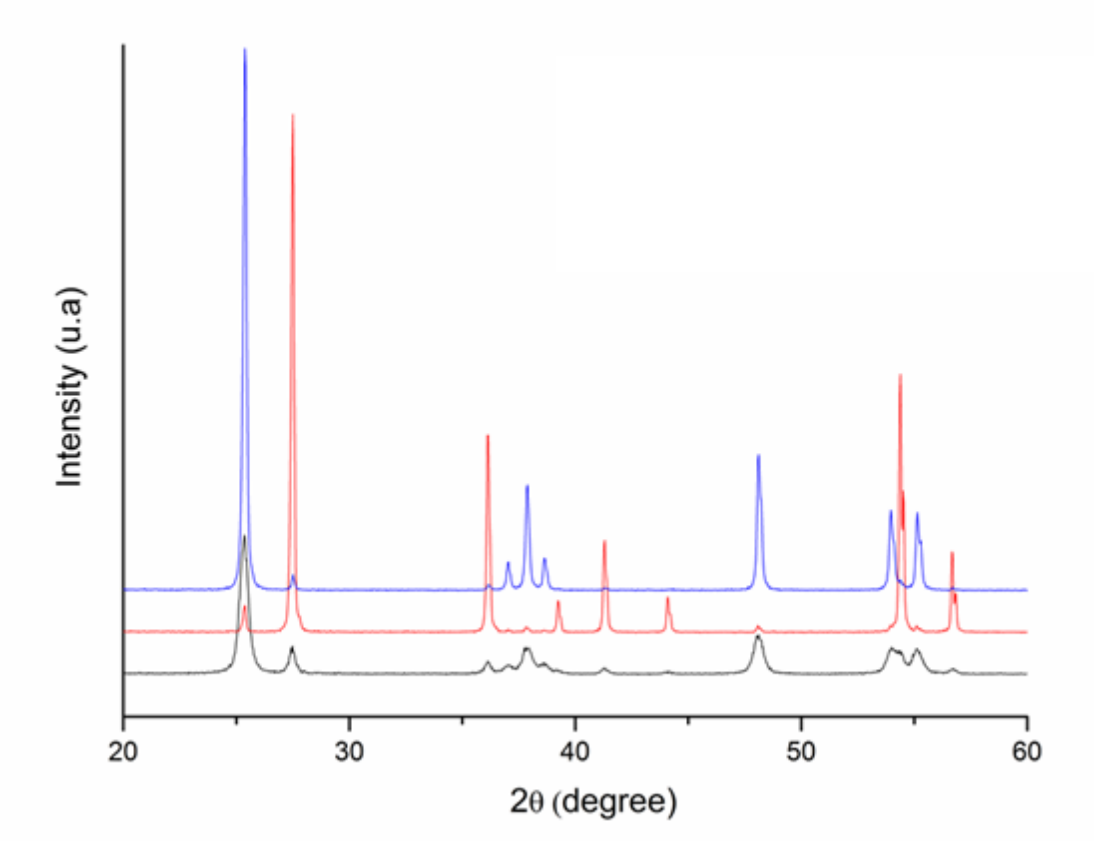

Fig.2 Representative STEM images of 0.1 wt% Au loaded on a) P25, b) anatase and c) rutile TiO_2

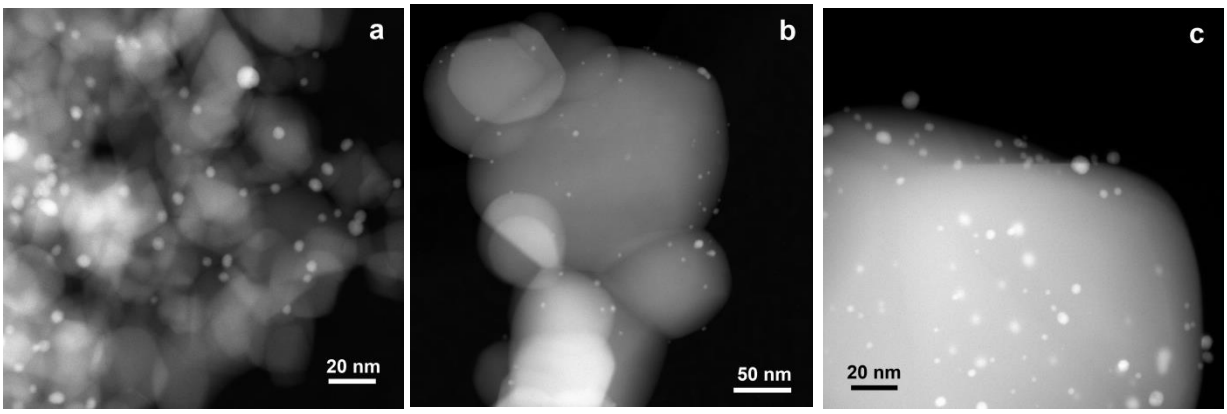

Fig.3 Representative HRTEM images of 0.1 wt% Au loaded on a) P25, b) anatase and c) rutile TiO_2

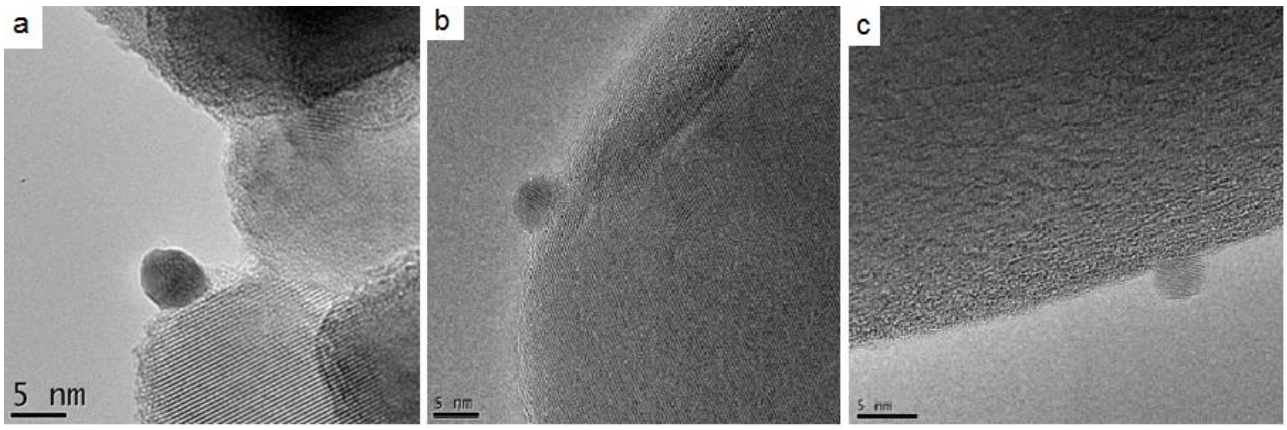

Fig. 4: DR-UV-Vis analysis of the 0.1 wt% Au/TiO_2 samples.

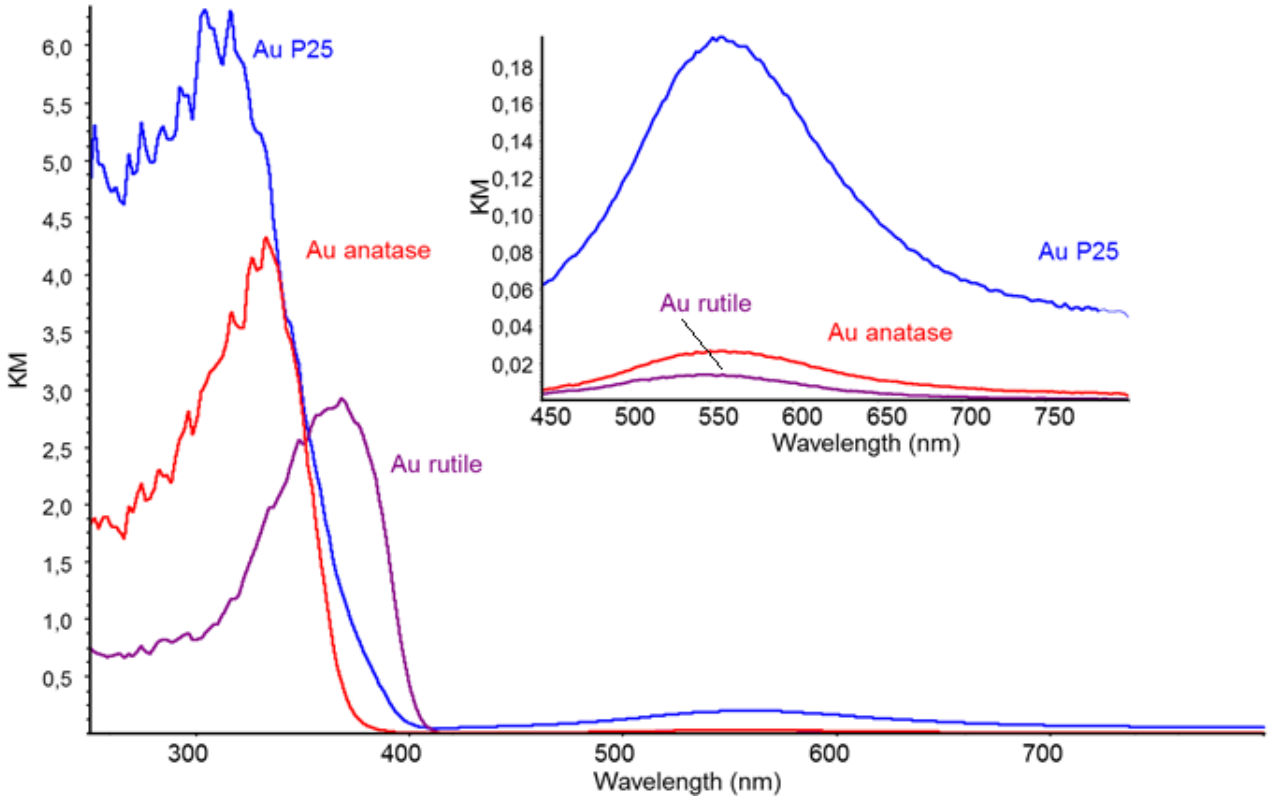

Fig. 5: Effect of saturation temperature and pressure on the equilibrium CO_2 molar fraction in water.

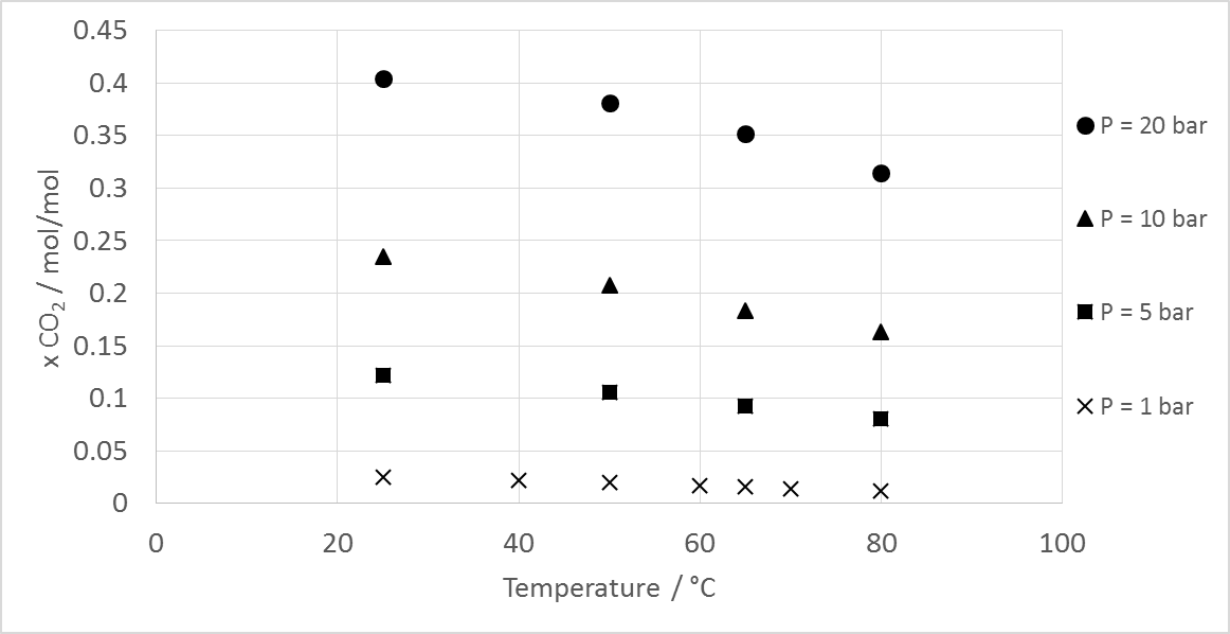

Fig. 6: Effect of CO_2 saturation and reactor pressure on H_2 (full triangles) and CH_4 (circles) productivity at pH = 11.4, T = 65°C. H_2 productivity (empty triangles) at pH 5.5, T = 65°C. Sample 0.1 wt% Au/P25.

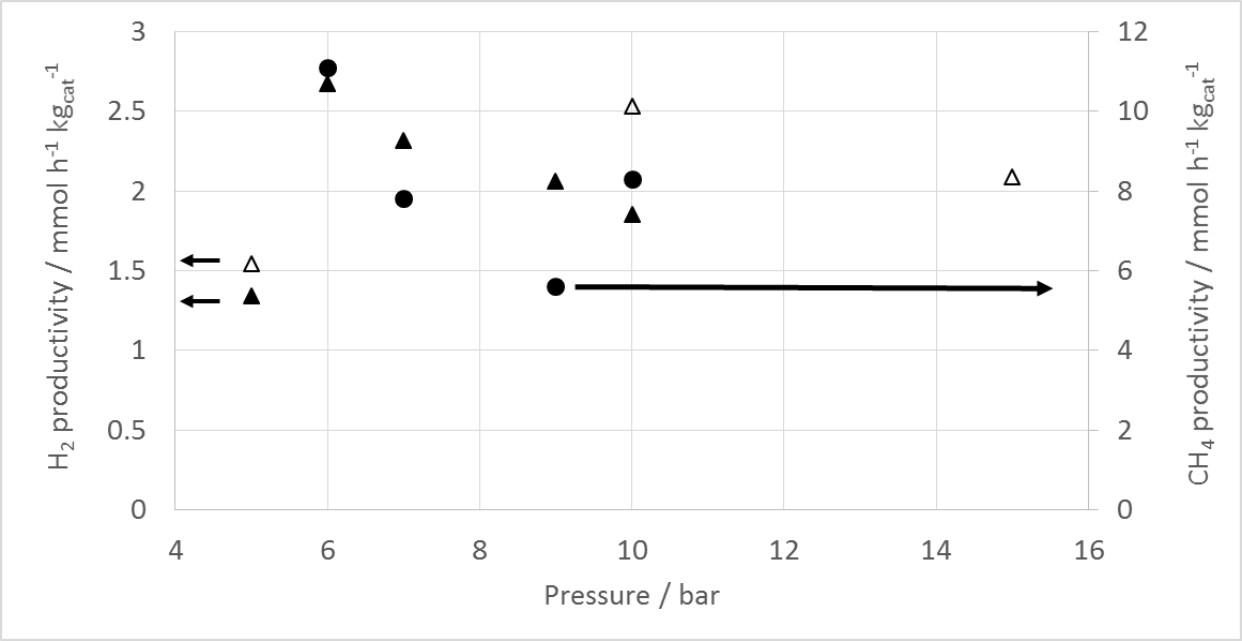

Fig. 7: Effect of reaction temperature on H_2 (triangles) and CH_4 (circles) productivity at pH = 5.5 and 11.4, P = 5 bar, sample 0.1 wt% Au/P25.

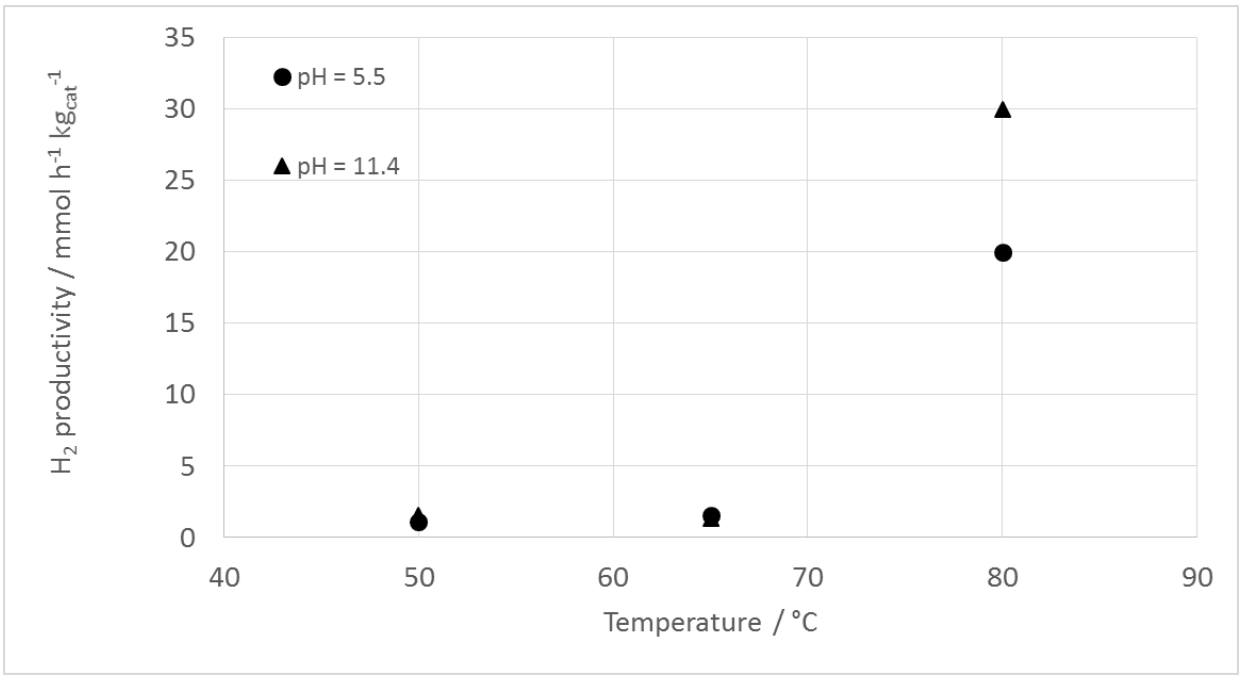

Fig. 8: Effect of TiO_2 structure on H_2 and CH_4 productivity in gas phase and of liquid phase organic products at pH = 11.4, P = 6 bar, T = 65°C.